Hindawi
Advances in Polymer Technology
Volume 2023, Article ID 2758621, 6 pages
https://doi.org/10.1155/2023/2758621

Research Article

Fabrication and Mechanical Properties of Chitosan/FHA Scaffolds

Majid Salehi [1,2,3] **and Sahar Molzemi** [4]

[1]*Department of Tissue Engineering, School of Medicine, Shahroud University of Medical Sciences, Shahroud, Iran*
[2]*Sexual Health and Fertility Research Center, Shahroud University of Medical Sciences, Shahroud, Iran*
[3]*Tissue Engineering and Stem Cells Research Center, Shahroud University of Medical Sciences, Shahroud, Iran*
[4]*Student Research Committee, School of Medicine, Shahroud University of Medical Sciences, Shahroud, Iran*

Correspondence should be addressed to Sahar Molzemi; saharmolzemi@yahoo.com

Received 6 February 2023; Revised 25 April 2023; Accepted 8 June 2023; Published 4 July 2023

Academic Editor: Jindan Wu

Fluor-hydroxyapatite (FHA) is a biomaterial with dental and orthopedic potential that is highly regarded as a result of bioactivity and high biocompatibility. Chitosan is used as a growth promoting agent in the tissues of the tooth and bone. Composite scaffold from these biomaterials is used as a pattern of natural bone and tooth grafts in tissue engineering. In this study FHA was synthesized through coprecipitation method. Then chitosan/FHA composites with different amounts of FHA (15 and 30 wt%) were prepared via freeze drying way. Structural and physical characteristics of the scaffolds were determined by powder X-ray diffraction (XRD), Fourier transform infrared spectroscopy (FTIR) spectra, and morphological properties of the scaffolds were investigated using SEM evaluation. The compressive strength, water-uptake capacity, and biodegradation behavior of scaffolds were performed, as well. The results indicated that chitosan/30%FHA scaffold showed more compressive strength, lower biodegradation in phosphate buffer solution after 4 weeks. Therefore, it might be a suitable scaffold for tooth engineering.

1. Introduction

Composites of calcium phosphates and natural biopolymers are widely used as biomaterials for bone tissue repair and engineering [1–4].

Calcium phosphate (CP) is well-known as the basic substance for human hard tissue. A lot of researches have been conducted on CP-based biomaterials which they have led to creation of hydroxyapatite. Hydroxyapatite (HA, $Ca_{10}(PO_4)_6(OH)_2$) is the most important ingredient of bone and it is approximately consisting 69% of bone weight. It shows bioactivity and biocompatibility properties and it is used in bone grafts, dental implants, etc. [5–7]. Hydroxyapatite (HA) is the most important inorganic phase in hard tissue of mammals and other organisms. It is well known that HA crystallites in different parts of a living body have different morphological characteristics, depending on their specific function. For instance, their average size can vary from 20 to 40 nm long and 1 to 5 nm wide in bone up to several microns in extent in the dentin.

By replacing the fluoride ions with hydroxyl ions in calcium phosphate structures, a new material is created that is called fluorapatite (FA, $(Ca_5(PO_4)_3F)$). When it is compared with HA, it has higher mechanical and biological properties and thermal stability (melting point = 1650°C). Due to the smaller and equal fluoride ions, their placement in calcium phosphate structure is better than hydroxyl ions. Consequently, FA is more changeless and it is less dissoluble than HA. FA improves the cell activity and it is used in biomedical applications and it can be a good alternative for HA [8].

Scaffolds for bone tissue engineering, which are a promising approach for the treatment of defective and lost bone, are required to have osteoconductivity and biodegradability in addition to their three dimensional (3D) interconnected porous networks. It has been indicated that a scaffold pore size in the range of 100–400 μm is favorable for cell colonization, proliferation, and penetration [9].

Chitosan (CS) is well-known to be excellent in biocompatibility, biodegradability, antimicrobial property, wound healing, cell proliferation, and tissue regeneration, is a linear polysaccharide composed of glucosamine and *N*-acetyl glucosamine with β, 1–4 glycosidic linkages; the latter is a moiety of glycosaminoglycans [10]. It is known that during the biomineralization processes living organisms are able to crystallize and deposit a wide range of minerals. Among them calcium phosphates which are produced in vertebrates not only in normal (bones, teeth) but also pathological (dental and urinary calculus and stones, atherosclerotic lesions) calcifications of tissues [11–13].

Since, the single component system cannot cover all the confidants of bone tissue therefore, improving multicomponent systems for bone tissue is important. The integration of calcium phosphate particles, such as FHA, inside bioactive polymers such as the chitosan may potentially create multiphase biocomposites with the improved mechanical and biological response. In this paper, in order to combine the favorable biocompatibility of CS with the osteoconductivity of FHA, CS/FHA composites with favorable properties were prepared by freeze drying method. Then, their structural, mechanical, and physical properties were investigated, as well.

2. Experimental Details

2.1. Materials. The necessary materials for making the chitosan scaffold were obtained from Merck. These materials include: nano-fluorhydroxyapatite, calcium carbonate, ammoniumdihydrogen orthophosphate, ammonium fluoride.

2.2. Precipitation of FHA. Fluorhydroxyapatite was prepared by coprecipitation method as described by Shanmugam and Gopal [14]. About 3.96 g ammoniumdihydrogen orthophosphate was added in 125 ml of distilled water. Then, the pH of the solution was kept equal to 12 using amounts of ammonium hydroxide. After that, 0.5 g of ammonium fluoride was dissolved to phosphate solution as the fluoride source. The phosphate solution was added into 75 ml calcium solution with stoichiometric quantities under stirring conditions. The suspension was maintained for 4 hr. The obtained product was centrifuged, dried overnight at 80°C, and calcined in air at 750°C for 1 hr.

2.3. Preparation of Scaffolds. At first chitosan was dissolved in 50 ml of 20% acetic acid solution using a stirrer for 1 hr to obtain a homogeneous solution. Then, different amounts of synthesized fluorhydroxyapatite in Section 2.1, were slowly added into the separately chitosan solution, under stirring at 500 rpm and were maintained for 24 hr at room temperature Then, 0.25% (v/v) glutaraldehyde was added to the ratio of the prepared solution and stirred for about 2 hr. The resultant solution was prefrozen at −55°C for 2 hr and followed by freeze-drying at −80°C for 24 hr. According to amounts of wt% FHA, the prepared scaffolds were labeled CS/15FHA and CS/30FHA (Figure 1).

Figure 1: Prepared scaffolds of CS/FHA by freeze drying method.

2.4. Characterization. The X-ray diffraction (XRD) characterization of FHA and composites were investigated at ambient temperature; using a Bruker D8 diffractometer with Cu Ka radiation (40 kV and 30 mA). Fourier Transform Infrared Spectra (FTIR) is recorded in the range 4,000–400 cm^{-1} using Thermo 6700 model. Scanning electron microscopic images are recorded by VEGA TESCAN.

2.5. Mechanical Testing. To study the mechanical strength of Chitosan/15Fluor-hydroxyapatite (CS/15FHA) and Chitosan/30Fluor-hydroxyapatite (CS/30FHA) scaffolds, compressive strength, and young's modulus were conducted using the Universal. Next, the compressive pressure was employed by a testing machine (STM 400 Santam at a rate of 0.5 mm min^{-1} at ambient temperature and with a 0.2 kN load cell. The samples with a size of (10 and 12.5 mm in diameter and thickness, respectively) were used in the compressive property test.

2.6. Porosity Investigations. The porosity of scaffolds was considered by fluid displacement method [15]; therefore, hexane was used as the replacement liquid. The scaffolds pieces' size was $1 \times 1 \times 1.5$ cm and placed in a 10 ml graduated cylinder with a specific hexane volume (V_1). The hexane-impregnated scaffold volume was considered as V_2 and gained by the immersed scaffold in hexane for 1 hr. The volume difference ($V_2 - V_1$) represented the composite scaffold volume. V_3 was determined as the residual hexane volume in the graduated cylinder after the impregnated sample was eliminated from the cylinder. The hexane volume in the scaffold ($V_1 - V_3$), was known as the scaffold empty volume. Hence scaffold total volume was $V = (V_2 - V_1) + (V_1 - V_3) = V_2 - V_3$. The scaffold porosity (ε) was resulted as follows:

$$\varepsilon\,(\%) = \frac{(V_1 - V_3)}{(V_2 - V_3)} \times 100. \quad (1)$$

2.7. Water-Uptake Capacity. The scaffolds dry weight (CS/15FHA and CS/30FHA) was shown as W_d. Then, they were soaked in deionized distilled water overnight. In contrast, the scaffolds wet weight was shown as W_w. Eventually the scaffolds water-uptake capacity was measured as the following:

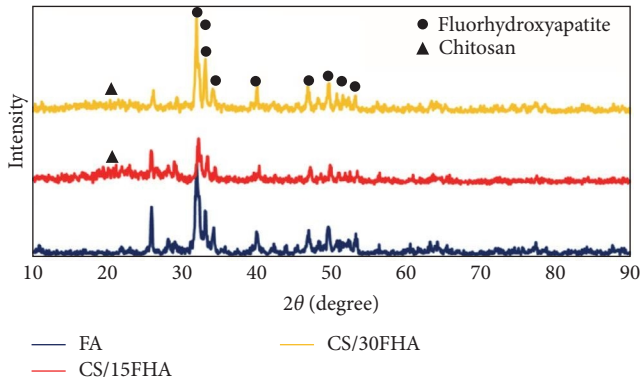

Figure 2: XRD analysis of pure FHA, CS/15FHA, and CS/30FHA scaffold.

$$\text{Water} - \text{uptake capacity}\,(\%) = \frac{(W_w - W_d)}{W_d} \times 100. \quad (2)$$

2.8. In Vitro Degradation. The degradation rate of fabricated scaffolds was measured in phosphate buffer solution (PBS) (pH: 7.4) and 37°C for 4 weeks. Each week, one scaffold was exited from PBS and washed in deionized distilled water to clean surface absorbed ions and then freeze-dried. The scaffolds initial weight was calculated as W_0 and the final weight after freeze drying was measured as W_D [16]. Finally, the degradation (%) was calculated based on the following:

$$\text{Degradation}\,(\%) = \frac{(W_0 - W_D)}{(W_0)} \times 100. \quad (3)$$

3. Results

3.1. Structural Characterization. X-ray diffraction patterns for the pure FAH, CS/15FAH, and CS/30FAH scaffolds, are shown in Figure 2. For pure FHA all appeared peaks at $2\theta = 26.06°, 31.97°, 32.36°, 33.14°, 34.25°, 40.48°, 46.98°$, and 49.52°, according to (211), (112), (300), (002), (213), (222), (202), and (310), crystalline plates, respectively, which are related to FHA formation in crystalline phase form. This result is in agreement with reported results previously [8]. The sharp diffraction peak at 2θ of 31.97° exhibited that FHA fabricated well-structure crystals [14]. All of the FHA peaks and CS peaks of CS/15FHA and CS/30FHA scaffolds, (2θ–20°) appeared successfully. These results are agreement with similar research [17]. However, with the increase in CS content (decrease in FHA content), the intensities of peaks decreased indicating of the lower crystallization of FHA in CS/15FHA than to CS/30FHA scaffold. The severity of CS peaks was simultaneously decreased as increasing of the FHA content increased, as well. The crystalline average size of FHA and FHA/CS composites based on (112) and (300) crystalline plates was estimated by Scherer equation:

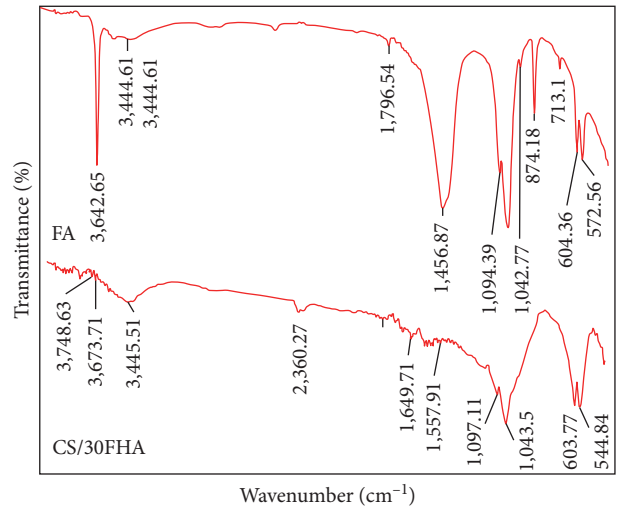

Figure 3: FTIR spectra of pure FHA and CS/30FHA scaffold.

$$D = \frac{K\lambda}{\beta \cos\theta}, \quad (4)$$

where D is the mean size of the ordered crystalline, K is a dimensionless shape factor, l is the X-ray wavelength, β is the line broadening at half of the maximum intensity (FWHM), and θ is the Bragg angle. According to Scherer equation, it can be concluded that the crystallite size of FHA is estimated about 14.6 nm and for both of scaffolds obtained 19.7 nm.

As it shown in Figure 3 the Fourier transform infrared spectroscopy absorption peaks of the FAH and CS/30FHA synthesized scaffolds were investigated in the 400–4,000 cm^{-1} range. The spectra display the characteristic vibrational modes corresponding to the apatite phosphate group (stretching (947–1,037 cm^{-1}) and bending vibrations (571–611 cm^{-1}) of P–O bond. The intensity peaks at 632 and 559 cm^{-1} attributed to $\gamma 4$ of phosphate, whereas the bands at 968 and 1,048 cm^{-1} were assigned to $\gamma 1$ of phosphate and $\gamma 3$ of the phosphate mode respectively [14, 17]. The FTIR spectrum of FAH indicates that stretching vibrations and bending modes of OH were observed at 3,445 and 632 cm^{-1}, respectively.

For the CS/30FHA scaffold could be characterized by broadening of the band at 1,050 cm^{-1} shows the presence of polymer and its interaction with the phosphate groups [8, 17]. The bands at 1,550–1,700 cm^{-1} are attributable to mode superposition of the hydroxyapatite OH group and the chitosan amide I and amide II groups. The bands at 3,400–3,700 cm^{-1} are attributed to the hydroxyl groups present in chitosan. The hydroxyapatite phosphate stretching (vibration) bands are at 1,000–1,100 cm^{-1} and the phosphate bending bands are at 500–600 cm^{-1} [18].

The CS/15FHA and CS/30FHA scaffolds SEM images are revealed in Figure 4. For both scaffolds, the number of interconnected pores are obvious. For the CS/15FHA, interconnected pores are higher compared to CS/30FHA. Therefore, FHA amount increasing (the decrease in CS content) in scaffold structure causes rougher pore walls which are proper for the cell attachment [17]. Also, the mean porosity and the

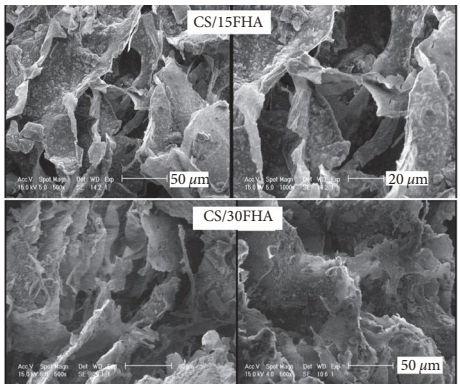

Figure 4: SEM images of CS/15FHA and CS/30FHA scaffolds.

interconnectivity of CS/FHA composite scaffolds were mostly influenced by the FHA amount. The porosity reduction resulted from the increasing amount of FHA since agglomeration of nHA occurred as pore walls become thicker [19]. Due to the intermolecular hydrogen bonding between NH_2 groups of CS and OH groups of FHA, the increase in FHA amount reduced porosities [20]. Therefore, SEM study of the CS/FHA scaffold stated that the microstructure provides a good microenvironment for tissue engineering.

3.2. Water-Uptake Capacity and Porosity Measurement. CS/FHA water-uptake and porosity investigations are shown in Figures 5(a) and 5(b). The composite scaffolds studies stated that the water retention capacity is more than the aboriginal weight and proper water-uptake capacity. The result revealed that the FHA addition (reduction in CS amount) decreased the CS/FHA scaffolds swelling. This may be attributed to cross-linked chains of FHA that decreased the hydrophilicity by the phosphate and calcium bonding to the hydrophilic groups of OH or NH_2 [21]. Water-uptake could develop the cell's permeation into the scaffolds by a 3D structure, during cell culture. Also, water-uptake increases the scaffolds pore size and total porosity.

Porosity measurement is vital for transporting oxygen and nutrients to the internal composite scaffolds bits. In fact, the cell proliferation rate was improved by scaffold surface adhesion. According to Figure 5(b), as the CS amount decreased from CS/15FHA to CS/30FHA, the porosities decreased from 61% to 40% as well. This was due to the FHA in the scaffold. By controlling the key freeze-drying parameters such as the cooling and temperature rate, could cause greater pore sizes due to the ice crystals growth that influenced the pore sizes [16].

3.3. Mechanical Properties. Appropriate mechanical characteristics of scaffolds contribute to the tissue restoration. Also, matrices mechanical properties affect cell behaviors substantially, e.g. adhernece, growth, and differentiation. In this study, the FHA insertion effect (increasing in the FHA or decreasing in CS amount) on the compressive strength (Figure 6) of the composite scaffolds was examined. The results revealed that mechanical strength of CS/FHA scaffolds changed as FHA amount increased (considering the decreasing in the CS amount). However, the scaffolds water uptake and porosity

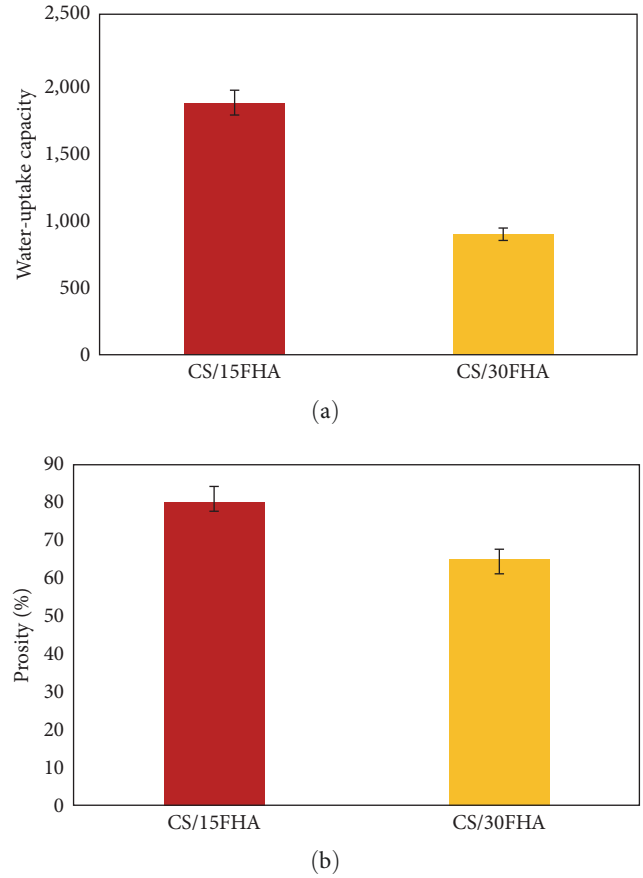

Figure 5: Water-uptake capacity and porosity of CS/15FHA and CS/30FHA scaffolds.

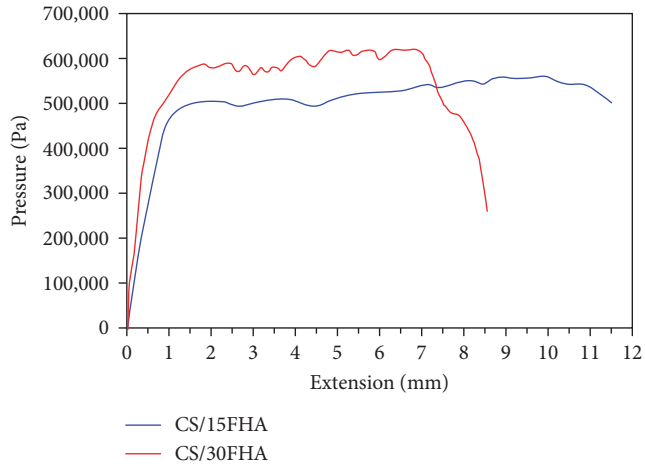

Figure 6: Compressive strength of CS/15FHA and CS/30FHA scaffolds.

may improve cell attachment, it could decrease its mechanical properties. As shown in Figure 6, the compressive strength of CS/30FHA is higher compared to CS/15FHA.

3.4. Biodegradation Behavior. Figure 7 reveals the degradation rate of various weight concentrations of CS/FHA composite scaffolds in PBS solution was studied for 4 weeks. A

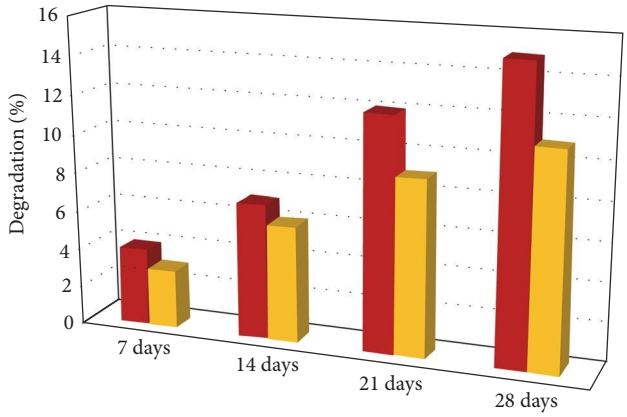

Figure 7: Biodegradation behavior of CS/15FHA and CS/30FHA scaffolds.

previous study stated that by increasing the degradation time, the macromolecules of the scaffold surface broke into small molecules (oligomer units) with preferential hydrolytic scission, which could be dissolved in PBS [22]. According to the results by FHA addition into the composite (the decreasing in CS), the scaffolds degradation value was reduced. Finally, after 4 weeks, every composite weight was reduced by 11%–15%. This proved that the degradation of the composite scaffold may be controlled by FHA and CS amounts which could be suitable for tissue engineering approaches.

4. Conclusions

In this study FHA nanoparticles with particle size of 14.6 nm was synthesized by coprecipitation method successfully. After that, CS/FHA scaffolds were fabricated by freeze drying in −80°C. The XRD results indicated that by increasing of CS (decrease in FHA) content in scaffolds, decreased the intensity of FHA crystalline peaks. Also according to SEM images enhancement of FHA leads to rougher pore walls and reduced interconnected pores which is the main reason of higher compressive strength of CS/30FHA than CS/15FHA scaffold. According to the results, with the incorporation of FHA into the composite (the decrease in CS), the degradation behavior, water-uptake capacity, and porosity change are controllable. Therefore, CS/FHA composite can be a desired candidate as a scaffold for tissue engineering.

Data Availability

All data including figures, tables, and experimental results are available.

Conflicts of Interest

The authors declare that they have no conflicts of interest.

Acknowledgments

Authors gratefully thank Nanonafez Company in Semnan University Science and Technology Park, Shahroud Branch Islamic Azad University, and Shahroud University of Medical Science and Department of Tissue Engineering, School of Medicine, Shahroud University of Medical Sciences, Shahroud, Iran, for supporting the research work.

References

[1] Z. Kang, X. Zhang, Y. Chen, M. Y. Akram, J. Nie, and X. Zhu, "Preparation of polymer/calcium phosphate porous composite as bone tissue scaffolds," *Materials Science and Engineering: C*, vol. 70, Part 2, pp. 1125–1131, 2017.

[2] M. Neumann and M. Epple, "Composites of calcium phosphate and polymers as bone substitution materials," *European Journal of Trauma*, vol. 32, pp. 125–131, 2006.

[3] B. Huang, G. Caetano, C. Vyas, J. J. Blaker, C. Diver, and P. Bártolo, "Polymer-ceramic composite scaffolds: the effect of hydroxyapatite and β-tri-calcium phosphate," *Materials*, vol. 11, no. 1, Article ID 129, 2018.

[4] A. Nandakumar, L. Yang, P. Habibovic, and C. van Blitterswijk, "Calcium phosphate coated electrospun fiber matrices as scaffolds for bone tissue engineering," *Langmuir*, vol. 26, no. 10, pp. 7380–7387, 2010.

[5] M. H. Fathi, A. Hanifi, and V. Mortazavi, "Preparation and bioactivity evaluation of bone-like hydroxyapatite nanopowder," *Journal of Materials Processing Technology*, vol. 202, no. 1–3, pp. 536–542, 2008.

[6] H. Ghomi, M. H. Fathi, and H. Edris, "Effect of the composition of hydroxyapatite/bioactive glass nanocomposite foams on their bioactivity and mechanical properties," *Materials Research Bulletin*, vol. 47, no. 11, pp. 3523–3532, 2012.

[7] C. V. Ragel, M. Vallet-Regí, and L. M. Rodríguez-Lorenzo, "Preparation and in vitro bioactivity of hydroxyapatite/solgel glass biphasic material," *Biomaterials*, vol. 23, no. 8, pp. 1865–1872, 2002.

[8] B. Nasiri-Tabrizi and A. Fahami, "Synthesis and characterization of fluorapatite-zirconia composite nanopowders," *Ceramics International*, vol. 39, no. 4, pp. 4329–4337, 2013.

[9] G. Turnbull, J. Clarke, F. Picard et al., "3D bioactive composite scaffolds for bone tissue engineering," *Bioactive Materials*, vol. 3, no. 3, pp. 278–314, 2018.

[10] A. Ehterami, N. R. kolarijani, S. Nazarnezhad, M. Alizadeh, A. Masoudi, and M. Salehi, "Peripheral nerve regeneration by thiolated chitosan hydrogel containing taurine: In vitro and in vivo study," *Journal of Bioactive and Compatible Polymers*, vol. 37, no. 2, pp. 85–97, 2022.

[11] J. P. Quiñones, H. Peniche, and C. Peniche, "Chitosan based self-assembled nanoparticles in drug delivery," *Polymers*, vol. 10, no. 3, Article ID 235, 2018.

[12] S. V. Dorozhkin and M. Epple, "Biological and medical significance of calcium phosphates," *Angewandte Chemie International Edition*, vol. 41, no. 17, pp. 3130–3146, 2002.

[13] S. V. Dorozhkin, "Calcium orthophosphates in nature, biology and medicine," *Materials*, vol. 2, no. 2, pp. 399–498, 2009.

[14] S. Shanmugam and B. Gopal, "Copper substituted hydroxyapatite and fluorapatite: synthesis, characterization and antimicrobial properties," *Ceramics International*, vol. 40, no. 10, Part A, pp. 15655–15662, 2014.

[15] R. Jayakumar, K. P. Chennazhi, S. Srinivasan, S. V. Nair, T. Furuike, and H. Tamura, "Chitin scaffolds in tissue engineering," *International Journal of Molecular Sciences*, vol. 12, no. 3, pp. 1876–1887, 2011.

[16] L. Ghorbanian, R. Emadi, S. M. Razavi, H. Shin, and A. Teimouri, "Fabrication and characterization of novel diopside/silk fibroin

nanocomposite scaffolds for potential application in maxillofacial bone regeneration," *International Journal of Biological Macromolecules*, vol. 58, pp. 275–280, 2013.

[17] Z. Shahbazarab, A. Teimouri, A. N. Chermahini, and M. Azadi, "Fabrication and characterization of nanobiocomposite scaffold of zein/chitosan/nanohydroxyapatite prepared by freeze-drying method for bone tissue engineering," *International Journal of Biological Macromolecules*, vol. 108, pp. 1017–1027, 2018.

[18] S. N. Danilchenko, O. V. Kalinkevich, M. V. Pogorelov et al., "Chitosan-hydroxyapatite composite biomaterials made by a one step co-precipitation method: preparation, characterization and in vivo tests," *Journal of Biological Physics and Chemistry*, vol. 9, no. 3, pp. 119–126, 2009.

[19] V. Karageorgiou and D. Kaplan, "Porosity of 3D biomaterial scaffolds and osteogenesis," *Biomaterials*, vol. 26, no. 27, pp. 5474–5491, 2005.

[20] M. Escamilla-García, G. Calderón-Domínguez, J. J. Chanona-Pérez et al., "Physical and structural characterisation of zein and chitosan edible films using nanotechnology tools," *International Journal of Biological Macromolecules*, vol. 61, pp. 196–203, 2013.

[21] J. Li, Y. Dou, J. Yang et al., "Surface characterization and biocompatibility of micro- and nano-hydroxyapatite/chitosan-gelatin network films," *Materials Science and Engineering: C*, vol. 29, no. 4, pp. 1207–1215, 2009.

[22] B. A. C. Harley, H.-D. Kim, M. H. Zaman, I. V. Yannas, D. A. Lauffenburger, and L. J. Gibson, "Microarchitecture of three-dimensional scaffolds influences cell migration behavior via junction interactions," *Biophysical Journal*, vol. 95, no. 8, pp. 4013–4024, 2008.